Human Molecular Genetics, 2004, Vol. 13, No. 22 **2813–2821**
doi:10.1093/hmg/ddh307
Advance Access published on September 22, 2004

Heightened susceptibility to chronic gastritis, hyperplasia and metaplasia in *Kcnq1* mutant mice

Colleen M. Elso[1], Xiaochen Lu[1], Cymbeline T. Culiat[2], Joe C. Rutledge[3], Nestor L.A. Cacheiro[2], Walderico M. Generoso[2] and Lisa J. Stubbs[1,*]

[1]Genome Biology Division, Lawrence Livermore National Laboratory, Livermore, CA 94550, USA, [2]Life Sciences Division, Oak Ridge National Laboratory, Oak Ridge, TN 37831, USA and [3]Department of Laboratory Medicine, Children's Hospital, Seattle, WA 98105, USA

Received July 13, 2004; Revised and Accepted September 15, 2004

Increased susceptibility to gastric cancer has been associated with a wide range of host genetic and environmental factors, including *Helicobacter pylori* infection. *Helicobacter pylori* infection is postulated to initiate a progression through atrophic gastritis, metaplasia and dysplasia to cancer, and has been associated with reduction of acid output and dysregulation of stomach mucins. Here, we present the characterization of two mouse lines carrying mutant alleles of the gene encoding the Kcnq1 potassium channel, which very rapidly establish chronic gastritis in a pathogen-exposed environment. These mice develop gastric hyperplasia, hypochlorhydria and mucin dysregulation independent of infection. Metaplasia, dysplasia and premalignant adenomatous hyperplasia of the stomach have been observed in these *Kcnq1* mutant mice, also independent of infection. The data presented here suggest that *Kcnq1* mutant mice can be used both as an efficient model for the development of atrophic gastritis after infection and to determine the processes during the later stages of progression to gastric cancer independent of infection. Thus, *Kcnq1* mutant mice are a powerful new tool for investigating the connection between acid balance, *Helicobacter* infection and mucin disruption in the progression to gastric cancer.

INTRODUCTION

Gastric cancer is a leading cause of cancer-related death. Both host genetic and environmental factors are known to influence the induction of gastric cancer, but currently no clear set of conditions have been defined (reviewed in 1,2). It has been established that infection with *Helicobacter pylori* is associated with an increased risk of gastric adenocarcinoma in humans. The progression to the most well studied 'intestinal' form of gastric cancer is thought to follow a specific program beginning with *H. pylori* infection and accompanying gastritis which results in the loss of parietal cells. The mechanism for the progression to metaplasia and cancer that follows this atrophic gastritis is unclear. Two possibilities are that *H. pylori* could be initiating direct cellular damage through an increase in oxidative species (3), or that hypochlorhydria due to glandular atrophy may allow an increase in carcinogenic compounds in the stomach, possibly enhanced through the action of opportunistic infecting bacteria (4). The complex interaction between host and environment leading to gastric cancer is a continuing focus of research.

A number of animal models have been developed for investigating the mechanism of *Helicobacter* infection and ensuing disease. Gastritis is a commonly recorded outcome in these models, but the progression to gastric cancer has been more difficult to reproduce. However, it is now known that gastric cancer, remarkably similar to that seen in humans, can be elicited through *Helicobacter* infection of the Mongolian gerbil (5). Mouse models involving infection with *H. pylori* and *H. felis* have also been developed (6,7), but wild-type mice are generally resistant to these *Helicobacter* infections, and protocols to establish them require repeated intragastric inoculation. The development of gastritis and more advanced disease states often require extremely long-term observations, and gastric adenocarcinoma is not commonly observed. Nevertheless, similarities to the human disease do exist, as mice

*To whom correspondence should be addressed. Tel: +1 9254228473; Fax: +1 9254222099; Email: stubbs5@llnl.gov

infected with *H. felis* develop MALT lymphoma after extended infection periods (8) and infection with *Helicobacter* can exacerbate the effects of agents already known to induce gastric cancer (9). Susceptibility to *Helicobacter* infection and its downstream effects in mice has been shown to have a genetic basis through the differential susceptibility of inbred lines (10), although contributing genetic factors have not been elucidated.

A growing amount of evidence in humans also supports a role for host genetics in determining susceptibility to gastric cancer (11,12). Human conditions associated with increased risk of gastric cancer commonly include phenotypes such as atrophic gastritis, hypertrophy and hypergastrinemia. For instance, Menetrier's disease is characterized by enlargement of the rugal folds, chronic atrophic gastritis of fundic glands, the presence of large cysts in the mucosa and overproduction of mucus (13). Another genetic condition, autoimmune gastritis, is associated with gastritis, atrophic fundic glands and hypergastrinemia (14). Moreover, polymorphisms in several genes, including those encoding inflammatory response proteins such as interleukin-1β and TNF, tumor suppressors, oncogenes and enzymes involved in the detoxification of carcinogens, the removal of oxidative species and repair of DNA damage have been associated with susceptibility to gastric cancer (reviewed in 11,12).

Several mouse mutations have recently been generated that partially recapitulate the features associated with the progression to gastric cancer. Lee *et al.* (15) have noted severe gastric hyperplasia due to expansion of the middle and neck cells in the gastric mucosa, accompanied by achlorhydria and hypergastrinemia in animals inheriting targeted mutations in the potassium channel gene, *Kcnq1*. *Kcnq1* has been localized to the parietal cells in the gastric glands of both mice and human and is required for normal acid secretion (16,17). Therefore, it is interesting to note that no aberrant stomach phenotype has been associated with *KCNQ1* mutations in humans. However, to the best of our knowledge, no studies specifically addressing gastritis in humans with *KCNQ1* mutations have been carried out and the pathology may be present at subclinical levels. Alternatively, there could be a difference between mouse and human K^+ regulation in parietal cells, with humans possibly having a compensatory mechanism not present in mouse. *KCNQ1* mutations have been associated with two human syndromes (18–20): Romano-Ward or Long QT syndrome (LQTS, OMIM: #192500) characterized by cardiac arrhythmias, and Jervell and Lange–Nielsen syndrome (JLNS, OMIM: #220400) involving profound bilateral deafness in addition to the cardiac phenotype. Translocations disrupting *Kcnq1* have also been associated with Beckwith–Wiedemann Syndrome (BWS, OMIM: #130650), a developmental disorder associated with alterations in imprinting of this region. A discussion of BWS in relation to our *Kcnq1* mutants is beyond the scope of this article.

Appropriate potassium balance provided through the action of *Kcnq1* is important for the function of the H/KATPase pump, which is responsible for the transfer of H^+ ions into the stomach. Disruption of either subunit of this pump results in achlorhydria and hypergastrinemia in the stomach (21–23). As expected, because of the functional interaction between these two proteins, disruption of the *H/KATPase* β gene results in stomach hyperplasia similar to that observed in *Kcnq1*−/− mice. Over-expression of gastrin can also induce hyperplasia of the stomach, and removal of gastrin by crossing the *H/KATPase* β deficient mouse with a gastrin deficient mouse reverses the hyperplastic phenotype (23). This implies that high levels of gastrin may be sufficient to induce the hyperplastic phenotype. On the other hand, *H/KATPase* α deficient mice which also have hypergastrinemia do not have stomach hyperplasia (22) and several other mouse models with hyperplastic stomachs do not have increased levels of gastrin (24,25). Therefore, the cause of the hyperplasia and the effect of gastrin in these mice are unclear. It is noteworthy that mice with induction of increased levels of gastrin are known to be at greater risk of gastric cancer (26).

Mucin dysregulation has also been associated with gastric cancer, and modification of gastric mucins to those more characteristic of the intestine is associated with a poor prognosis in humans (27). Disruption of the intestinal mucin gene, *Muc2*, in mice results in changes in crypt morphology and development of gastrointestinal cancers (28). A connection between mucin expression and *H. pylori* infection has also been noted. *Helicobacter pylori* can generate an imbalance of the mucin milieu in infected stomachs through the down-regulation of expression of the neutral mucin MUC5AC and spatial expansion of the expression of the acidic MUC6 from the base of the gland to the entire mucosa (29,30). Mucin dysregulation was also seen in H/KATPase α deficient mice (22), indicating that the acid level in the stomach may influence mucin expression.

In this report, we describe a mouse model that carries a balanced 7;10 reciprocal translocation and exhibits significantly increased susceptibility to gastritis in a pathogen-exposed environment. We also report the development of metaplastic and neoplastic changes and mucin dysregulation in the achlorhydric and hyperplastic stomachs of these mice, independent of exposure to pathogens. In addition, these mice display head bobbing and circling phenotypes accompanied by deafness, have enlarged hearts and reduced female fertility. We have determined that the gene disrupted by this translocation, and that is responsible for the phenotypes, is the potassium voltage-gated channel, subfamily Q, member 1 gene: *Kcnq1*. A second *Kcnq1* mutant 'vertigo-2' with similar phenotypes also displays gastric hyperplasia, and compound heterozygotes of the two mutations exhibit precancerous gastric lesions within 4 weeks of postnatal life. Our results suggest that these mutants will provide powerful new tools both for the study of *H. pylori*-dependent gastric cancer and for uncovering genetic factors that underlie cancer susceptibility in the absence of pathogens.

RESULTS

14Gso mice exhibit head bobbing and circling behavior, stomach hyperplasia, achlorhydria and dysregulated mucin expression

14Gso mice were identified in mutagenesis studies carried out at the Oak Ridge National Laboratory (ORNL) aimed at generating heritable reciprocal translocations in mice (31). The mutation in 14Gso was induced by X-ray irradiation of late

spermatids from a male founder mouse. Breeding studies identified mice carrying a reciprocal translocation that was associated with a recessive mutant phenotype characterized by head bobbing and circling behavior. Gross anatomical investigation revealed stomach hyperplasia and severe gastritis in these mice. Adult 14Gso mice exhibit increased stomach mass relative to body mass from ~1% in wild-type and heterozygous 14Gso mice to ~4% in homozygous 14Gso (T/T) mice ($P < 0.001$). The pH of the stomach contents was elevated to almost neutral conditions with 14Gso T/T mice ($N = 8$) having a stomach pH = 6.7 ± 0.13. In contrast, phenotypically normal T/+ mice ($N = 9$) have a stomach pH = 3.8 ± 0.37 (*t*-test: T/T versus T/+, $P = 4 \times 10^{-6}$). T/T mice also had a net reduction in acid secretion with an acid/base microequivalent per wet stomach mass of −13.9 ± 4.4 μEq/g in T/T mice ($N = 8$) and 25.0 ± 5.5 μEq/g in T/+ mice ($N = 8$) (*t*-test: T/T versus T/+, $P = 8 \times 10^{-5}$). Histological analysis of T/T 14Gso mice identified severe hyperplasia, and often disorganization, of the mucosa of the glandular region of the stomach, with frequent mucus filled cysts (Fig. 1A and B). The stomach hyperplasia had an early onset, with cytological manifestations observed even in 8-day-old neonates (Fig. 1E). These features were not seen in any other mice in the ORNL mutagenesis program including 3000 necropsied animals, representing litters from crosses of 200 translocation stocks (X. Lu, unpublished data). The region of mucosa which was expanded included both mucus neck cells and parietal cells, which often showed an abnormal morphology, characterized by the presence of many small vacuoles. PAS/Alcian blue staining indicated a dysregulation of mucin expression, as surface PAS staining was reduced in T/T 14Gso stomachs and both PAS and Alcian blue stainings were seen throughout the mucosa. Mucosal cysts were found to contain both neutral (PAS positive) and/or acidic (Alcian blue positive) carbohydrates (Fig. 1C and D).

14Gso mice are susceptible to gastritis in a pathogen-exposed environment

In a pathogen-exposed colony, a chronic inflammatory infiltrate [also known as mucosal associated lymphoid tissue (MALT)] was observed throughout the stomach mucosa of all T/T 14Gso mice (Fig. 1F). The onset of MALT was very rapid and was observed by 3 weeks of age in every pathogen-exposed 14Gso mutant mouse. This was not seen in normal or heterozygous littermates or cagemates or in any other animals screened in the ORNL mutagenesis study (L.J. Stubbs, C.T. Culiat and X. Lu, unpublished data). After re-derivation from frozen embryos and transfer of the mouse stock into a pathogen-free facility, the severe gastric inflammation was no longer evident (Fig. 1G). In aged animals in the pathogen-free environment, a low-grade chronic inflammation was observed with lymphocytes generally located beneath the mucosal layer. PCR detection of 16S rRNA gene and subsequent sequencing of the product showed that both normal control and 14Gso mutant mice from the pathogen-exposed colony, but not from the specific pathogen free colony, were infected with a range of bacteria including *Helicobacter*. The *Helicobacter* species was identified as *H. apodemus* by comparison of the sequence to the GenBank database.

14Gso mice exhibit stomach metaplasia and adenoma independent of infection

Histology of 32 stomachs from aged (12–21 months) T/T 14Gso mice, housed in a pathogen-free environment, showed the presence of squamous cell metaplasia in the hyperplastic region of the stomach in three cases (9% of T/T mice) (Fig. 1H). Regions of dysplasia were also observed (Fig. 1I). Abnormalities were not seen in any wild-type ($N = 20$) or T/+ ($N = 48$) 14Gso stomachs studied. Immunohistochemistry identified regions of p53- and carcino-embryonic antigen-positive staining. The staining was associated with both cuboidal epithelium surrounding dilated cysts and regions of dysplasia, containing cells with signet ring morphology, focal disorganization and increased ratio of nucleus to cytoplasm. These observations are indicative of pre-malignant adenomatous hyperplasia (Fig. 1K and L).

14Gso mice have inner ear defects and enlarged hearts

Histological investigation of the inner ear of T/T 14Gso mice revealed that the stria vascularis was reduced in thickness and the Reissner's membrane was collapsed onto the tectorial membrane, resulting in the reduction in size of the endolymph-containing scala media (unpublished data). The vestibular apparatus was also highly disorganized in structure. These observations explain the head-bobbing and circling behavior of the mutants, which is typical of animals with inner ear defects. The hearts of T/T 14Gso were enlarged compared with wild-type and T/+ controls. This was seen as an increase in mass and also an increase in ventricular wall thickness (unpublished data).

Kcnq1 is disrupted by the 14Gso Mmu7 translocation breakpoint

Initial karyotype analysis of 14Gso translocation carrier mice indicated a t(7;10)(F4;D) translocation. The translocation breakpoints are therefore located at the extreme distal tips of both chromosomes. To map the site of translocation more precisely, we selected bacterial artificial chromosome (BAC) clones at intervals surrounding the breakpoint region in Mmu7 to use as probes in FISH analysis. These experiments narrowed the 14Gso breakpoint into a region spanned by a single BAC clone, RPCI23-101n20 (Fig. 2). This BAC was completely occupied by exons of a large gene, encoding the potassium voltage-gated channel, subfamily Q, member 1 (*Kcnq1*). The *Kcnq1* transcription unit spans more than 320 kb of genomic sequence and the 2.8 kb transcript (NM_008434) has 16 exons (1α, 1–15). The RT–PCR analysis of RNA from homozygous 14Gso inner ear and stomach demonstrated that exons 1α, 1–9 of the *Kcnq1* mRNA are expressed, but consequent exons (10–15) could not be detected by RT–PCR (Fig. 3). These data indicated that a truncated *Kcnq1* transcript was synthesized in these mutant animals. The potassium pump and C-terminal association domains would be absent from the protein product of the disrupted gene thus resulting in a *Kcnq1* null allele. Immunohistochemical staining detected no Kcnq1 in parietal cells from mutant mice compared with strong staining in wild-type mice (Fig. 1M and N).

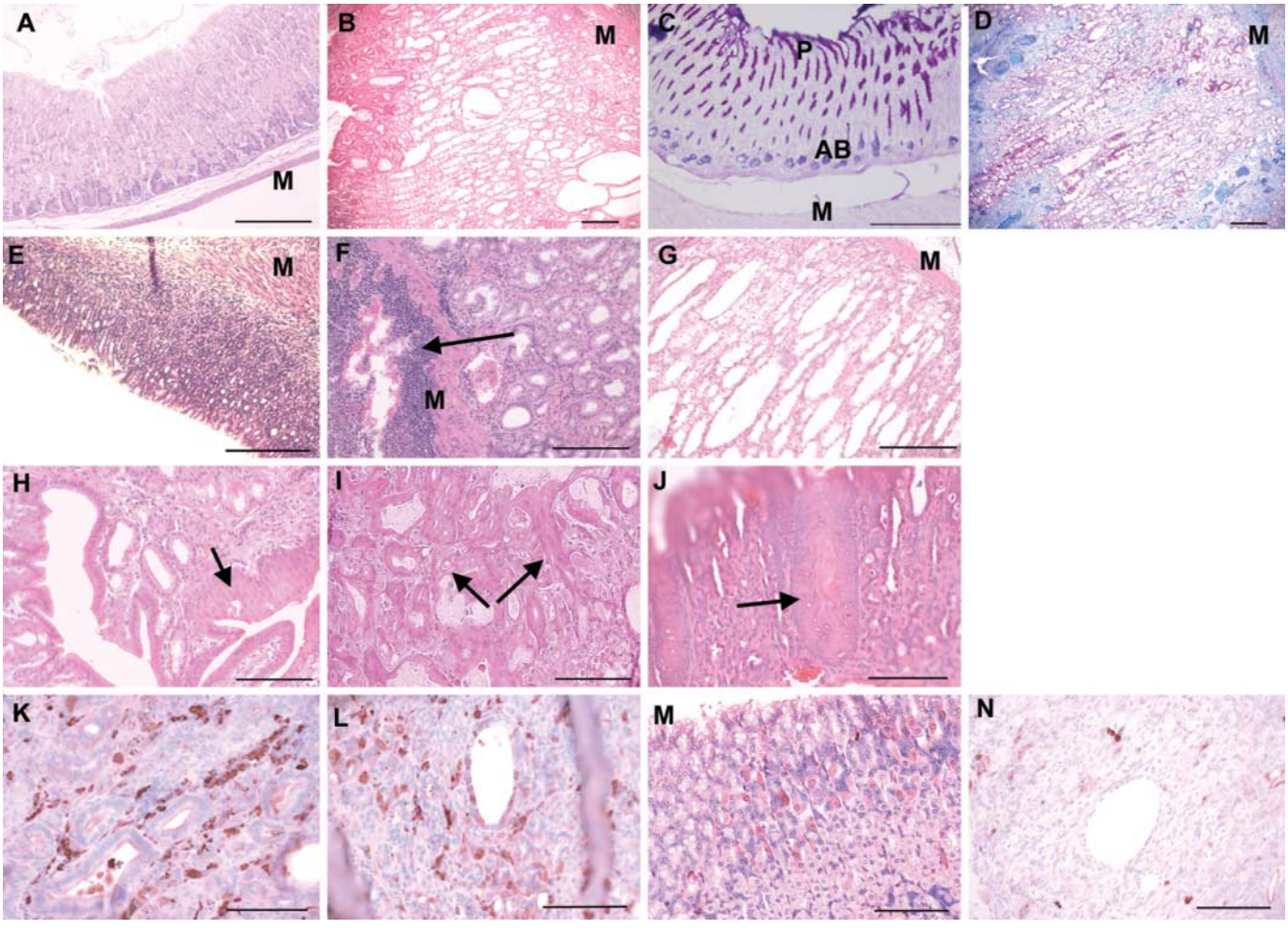

Figure 1. The increase in thickness of the mucosa and the presence of numerous cysts can be observed in hematoxylin and eosin-stained stomach sections from 14Gso T/T mice (**B**) compared with the wild-type control (**A**). PAS (P) and Alcian blue (AB) staining shows dysregulation of mucin expression in the mutant mice. In contrast to wild-type mice exhibiting strong PAS positive staining at the surface and Alcian blue positive staining at the base of the gland (**C**), Alcian blue staining is observed throughout the mucosa and there is a loss of PAS positive staining at the surface in 14Gso T/T mice (**D**). An increase in the width of the stomach mucosa is observed even at 8 days of age (**E**). A strong inflammatory infiltrate can be seen throughout the mucosa and under the muscle layer (arrow) of pathogen-exposed 14Gso T/T mice (**F**) but not of pathogen-free 14Gso T/T mice (**G**). Squamous cell metaplasia (arrow) is observed in stomach sections from aged 14Gso T/T mice (**H**). Dysplasia, seen as disorganization of the glandular structures (arrows) is observed in stomach section from a 14Gso T/T mouse (**I**). Squamous metaplasia (arrow) is observed in a 4-week-old compound heterozygote T/*vtg-2* mouse (**J**). Immunohistochemical staining of sections of 14Gso T/T stomach for cancer markers show positive staining of cells lining between glands (red). Antibodies: anti-carcinoembryonic antigen (**K**) and anti-p53 (**L**). Kcnq1 is absent from 14Gso mutant stomachs (**N**) compared with wild-type (**M**) where cells lining the glands are strongly stained. Bars: (A–G) 200 μm, (H–N) 100 μm. In (A–G) the position of the muscle layer at the base of the mucosa is indicated as M.

The RT–PCR data suggested that the Mmu7 translocation breakpoint was most likely located in intron 9 of the *Kcnq1* gene. Genomic PCR of overlapping 3 kb segments was performed using wild-type mouse and T/T genomic DNA samples as template to identify the location of the DNA rearrangement site. This method narrowed the region containing the breakpoint to a ∼3 kb interval in the mouse genome assembly 32 at contig NT_039437 (Fig. 4).

3′ RACE from *Kcnq1* identifies a fusion transcript and facilitates identification of the breakpoint sequence

Northern-blot analysis using a probe from the 5′ end of *Kcnq1* indicated that the *Kcnq1* transcript was larger than the predicted truncated product (unpublished data). We therefore suspected that the mutant *Kcnq1* transcript represents a fusion product extending across the translocation breakpoint and terminating in genetic material residing on Mmu10. Using 3′ RACE (32), a transcript that contained *Kcnq1* sequence extending to the end of exon 9 was recovered; however, the adjoining sequence most closely matched a genomic contig that had not been anchored to the mouse genome assembly (NT_083364.1). The gene prediction which was most closely aligned to the sequence was ‘similar to Cdc5-l’, (XM_135371), a presumed pseudogene. The 14Gso RACE sequences contained a local inversion of 826 bp compared with the genomic sequence in NT_083364.1. The breakpoints on both the Mmu7 : Mmu10 and Mmu10 : Mmu7 chromosomes

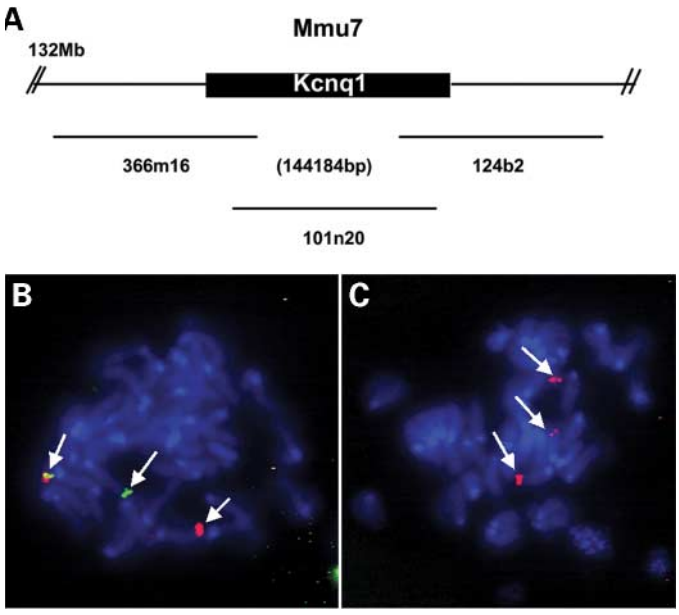

Figure 2. (**A**) Diagram depicting the three RPCI23 BACs which define the 14Gso Mmu7 breakpoint in relation to *Kcnq1*. (**B**) FISH analysis of 14Gso (T/+) metaphase chromosomes. RPCI23-366m16 (green) and RPCI23-124b2 (red) BACs are separated by the breakpoint. (**C**) RPCI23-101n20 BAC hybridizes to the wild-type chromosome 7 as well as both translocation chromosomes indicating the breakpoint lies within the sequence on that BAC.

were characterized by PCR and sequenced. Deletions of 5 bp at the breakpoint on Mmu7 and 11 bp on Mmu10 were found. There was also an ambiguous 2 bp which could be assigned to either chromosome, and 2 bp were duplicated at the position of the inversion (Fig. 4). FISH mapping localized the breakpoint on Mmu10 to BAC RPCI23-210k22 which was found to hybridize to both translocation chromosomes (unpublished data). This BAC lies in a poorly assembled region of the mouse genome, however, through alignment of rat and human genomic sequence with available genomic mouse sequence, sequence contig NT_083364.1 was assigned to this region (unpublished data). Many copies of the 'similar to Cdc5-l' sequence are found in the mouse draft sequence, suggesting this pseudogene has duplicated frequently and is distributed at many sites. Southern blotting and PCR confirmed that the breakpoint-spanning BAC contains several similar copies of this sequence (unpublished data). The 3′-terminus of the *Kcnq1* fusion transcript therefore lies within an Mmu10 copy of the *Cdc5l* pseudogene.

Characterization of the C3H/HeJCrl-Kcnq1$^{vtg\text{-}2J}$/J or 'vertigo-2' mouse

The vertigo-2 (*vtg-2*) mouse carries a spontaneous mutant allele of *Kcnq1*, and homozygous animals exhibit head tossing/circling and deafness similar to 14Gso mice (Gagnon *et al.*, Mouse Mutant Resource Website article. MMR/Kcnq1, http://www.jax.org/mmr/MMR_Remutation_vtg-2J.html). We examined this mutant to determine whether phenotypes associated with the 14Gso translocation were recapitulated in a

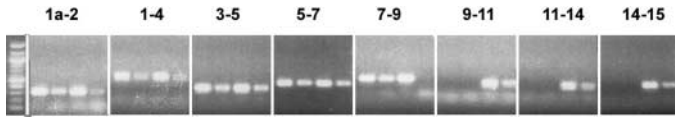

Figure 3. RT–PCR demonstrating expression of *Kcnq1* in 14Gso T/T stomach and ear mRNA (lanes 1 and 2 of each set of four) and wild-type stomach and ear mRNA (lanes 3 and 4 of each set of four). Exons analyzed in each set of four lanes are indicated above. A product is not seen for 14Gso T/T mRNA beginning from exon 9. NB: Exons 7–9 were amplified successfully from wild-type ear mRNA in repeat experiments.

second, independent *Kcnq1* mutant strain. Pathology studies of *vtg-2*/*vtg-2* animals demonstrated that this mutant also exhibits a form of stomach hyperplasia very similar to that seen in 14Gso mice. Female *vtg-2* mice are able to breed but do not care for their litters. As the *vtg-2* mutation had not been characterized on the molecular level, we generated RT–PCR products corresponding to different regions of the *Kcnq1* transcript from cDNA prepared from stomach and inner ear of homozygous *vtg-2* mice. We detected *Kcnq1* transcripts expressed from exon 2 to the end of the gene, but a product from exon 1α to exon 2 of the locus was not detected (Fig. 5A). Using 5′ RACE we were able to identify an intracisternal-A-particle (IAP)-transposable element inserted into *Kcnq1* exon 2 in *vtg-2* mice, providing an alternative starting codon and producing the 5′ truncated transcript (Fig. 5B). This 5′ truncated transcript potentially encodes a protein missing the first transmembrane domain of the subunit. Northern blot confirmed that there was also a minor long transcript, and long range RT–PCR confirmed that this began at exon 1α and read through the IAP element. A functional protein is not predicted from this transcript. Sequencing revealed that the terminus of the IAP was flanked by 5 bp of duplicated exon 2 sequence (unpublished data).

Allelic complementation analysis

A 14Gso T/T male was mated to a *vtg-2*/+ female, resulting in a litter of eight pups. Six of these pups, corresponding to compound heterozygotes, showed the head bobbing and circling phenotype. Histological analysis of stomachs from these mice at 4 weeks of age revealed hyperplasia and incidences of squamous metaplasia (Fig. 1J), compared with littermates heterozygous for the 14Gso translocation, which are normal. These results confirmed that the disruption of *Kcnq1* was sufficient to induce the behavioral (and therefore ear) phenotype, as well as stomach hyperplasia and metaplasia which we have documented in 14Gso mutant mice. Compound heterozygotes also displayed altered PAS/Alcian blue staining similar to that seen in 14Gso T/T mice (unpublished data).

DISCUSSION

We have described the phenotype and molecular basis of two novel mutations that disrupt the *Kcnq1* potassium channel gene. The t(7;10)14Gso translocation and the *Kcnq1*$^{vtg\text{-}2J}$ allele are both associated with inner ear defects and behavioral phenotypes observed in the previously reported *Kcnq1* deficient mice (15,33). The ear and cardiac phenotypes observed in 14Gso are essentially identical to those described

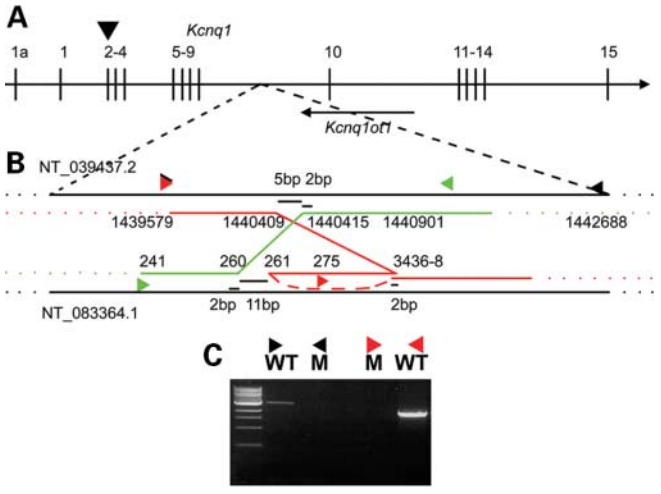

Figure 4. (**A**) Diagram indicating the exon structure of *Kcnq1* and the position of *Kcnq1ot1* in relation to the 14Gso Mmu7 breakpoint. The position of the *vtg-2* insertion is indicated by an arrowhead. (**B**) Diagram depiction of the 14Gso translocation. In red is the Mmu7 : 10 chromosome and in green is the Mmu10 : 7 chromosome. Black arrows indicate primers used to define the minimal breakpoint region on Mmu7 by PCR. Red and green arrows indicate primers used to amplify 14Gso DNA in order to determine the breakpoint sequence. Ethidium bromide stained PCR products are shown (**C**). Note that a product is produced from wild-type (WT), but not from mutant (M), genomic DNA with the first set of primers and the opposite with the second set. The size of deletions and overlaps are indicated. The inversion is represented by a dashed line.

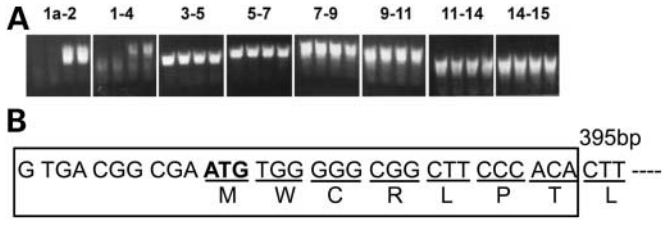

Figure 5. (**A**) RT–PCR demonstrating expression of *Kcnq1* in stomach and inner ear of *vtg-2/vtg-2* (lanes 1 and 2 of each set of four) and wild-type (lanes 3 and 4 of each set of four) mice. Exons analyzed in each set of four lanes are indicated above. No product was seen for exons 1α–2 and 1–4. (**B**) Sequence obtained from 5′ RACE preceding base pair 395 from *Kcnq1* sequence NM_008434. Sequence inside the box corresponds to an IAP transposable element. The inframe start codon is shown in bold text.

for *Kcnq1* targeted null mutations and were therefore not pursued further in this study. The mucosal hyperplasia with disorganized fundic glands, altered mucin expression and achlorhydria noted in *Kcnq1* knockout mice (15) was also observed in both 14Gso and *Kcnq1*$^{vtg\text{-}2J}$ mutant animals, confirming that the shared array of phenotypes results from disruption of *Kcnq1*. In addition, we reveal the novel observation that *Kcnq1* mutations predispose to metaplastic and pre-neoplastic changes in the stomachs of mutant mice. This has not been previously reported as most pre-neoplastic changes observed in *Kcnq1* mutant animals raised in a pathogen-free environment were detected in aged mice, and previous authors have focused primarily on analysis of younger mutant mice (15,33).

Over 100 mutations in *KCNQ1* have been found in families affected with LQTS and JLNS (LQT1 mutation database, http://pc4.fsm.it:81/cardmoc/). The majority of mutations in the dominant LQTS are missense mutations acting in a dominant negative manner. On the other hand, JLNS mutations act recessively and are more likely to be frameshift mutations acting to truncate the gene before the 'C-terminal assembly domain (CAD)'; so, the mutant subunits are not able to form associations with wild-type subunits (34,35). The 14Gso mutation truncates *Kcnq1* well before the CAD, and therefore falls into the class of mutations similar to those associated with JLNS. Conversely, the mutation in the *Kcnq1*$^{vtg\text{-}2}$ mouse, which also shows a recessive phenotype, retains the CAD; so, the mutant protein is therefore presumably able to associate with wild-type subunits. An N-terminal domain also required for subunit association has been suggested previously and could explain the recessive nature of this mutation (34). A number of other possibilities exist: the insertion of the IAP transposable element could cause a change in regulation or stability of the transcript. It is also possible that transport of the truncated protein could be affected. Further testing will be required to determine the mechanism of this mutation.

In addition to the adenomatous hyperplasia observed in 14Gso animals in an SPF environment, the mutants were also acutely susceptible to gastritis, or infiltration of the mucosa with MALT, when exposed to pathogens. MALT has been associated with infection with *H. pylori* in humans, as well as long-term infection with *H. felis* in mice (8,36). In the absence of pathogens, MALT is not seen in 14Gso mice, indicating that the induction of gastritis requires the environmental stimulus of infection. A number of bacterial species including a *Helicobacter* species with 16S rRNA sequence most similar to *H. apodemus*, an isolate first described in field mice, were detected in the stomachs of 14Gso mice in the pathogen-exposed environment. As other bacteria were also present, this does not prove that the MALT is an abnormal response to *Helicobacter* in these mice. However, the similarity between the response of these mice and that of animals purposely infected with *H. felis* (8) leaves the possibility that this may be the case.

Because similar responses were never observed in normal or carrier littermates, or control animals housed in the same conditions, we hypothesize that the achlorhydric stomach in 14Gso mice promoted infection with *Helicobacter* and/or other opportunistic pathogens, eliciting the marked inflammatory response by 3 weeks of age. These data suggest that the *Kcnq1* mutation in 14Gso mice provides a genetic background that will facilitate the very efficient study of the progression of *Helicobacter*-associated disease without the need for prolonged studies of chronic disease. Aside from the time required, these long-term studies can also be confounded by normal aging processes in the animal. Our observations also suggest an interesting set of hypotheses regarding genetic factors that might contribute to *H. pylori* infectivity and cancer susceptibility in humans.

Infection with *H. pylori* is a major risk factor for gastric carcinoma in human patients (reviewed in 1,2). The progression to cancer is thought to follow a specific program: infection; gastritis; atrophic gastritis; metaplasia and dysplasia; cancer. Our studies demonstrate that although the 14Gso mouse

is acutely susceptible to gastritis, this step is not required for the progression to cancer. Consequently, something intrinsic to the 14Gso system must be responsible for the observed adenomatous hyperplasia. Achlorhydria and hypergastrinemia, which are features of the progression from atrophic gastritis to metaplasia and dysplasia and ultimately cancer, both could be contributing to this progression. With the caveat that different mechanisms could be important in the development of cancer in humans and mice, this strain could be used to model these later stages of progression to gastric cancer and will allow the dissection of underlying genetic factors independent of infection.

Interestingly, in the light of the known connection between *H. pylori* infection and mucin dysregulation, an abnormal mucin balance was also observed in 14Gso mice. The reduction in intensity of staining of neutral mucin (presumably Muc5ac) and increase in the range of expression of acidic mucin (most likely Muc6, although the presence of Muc2 due to the development of intestinal metaplasia has not been ruled out) in 14Gso mice is reminiscent of the alterations described in response to *H. pylori* infection (30). Although infection may hasten the rate at which mucin dysregulation occurs in 14Gso mice, mucin imbalance also occurs independently of infection. As *Muc2* null mutations display a form of hypertrophy in the glandular cells of the colon that very closely resembles that seen in pathogen-free 14Gso mice, we speculate that mucin imbalance *per se* might play a critical role in hypertrophy that develops in both *Kcnq1* and *H/KATPase* mutations. Whatever the mechanisms underlying the pathology we have observed in 14Gso and *Kcnq1*$^{vtg\text{-}2}$ mice, these data indicate that *Kcnq1* mutations can be used as efficient new tools for investigating the connection between acid balance, *Helicobacter* infection, and mucin disruption in the progression to gastric cancer.

MATERIALS AND METHODS

Mice

The 14Gso mouse line was generated in the conventional mouse facility at Oak Ridge National Laboratory and was subsequently moved to a specific pathogen-free animal facility at Lawrence Livermore National Laboratory. Re-derivation of 14Gso was conducted from frozen embryos at the Charles River laboratories. The translocation was maintained on a B6C3 (C57BL/6 × C3H/He) background. Mice homozygous for the translocation could be identified before weaning due to head bobbing and circling behavior. Homozygous mutant males were bred to carrier or wild-type females to maintain the line. Mutants were present at an equivalent gender ratio. Homozygous mutant females were variable in their ability to breed and few were able to care for a litter. C3H/HeJCrl-*Kcnq1*$^{vtg\text{-}2J}$/J mice were obtained from The Jackson Laboratory.

Pathology and immunohistochemistry

Stomach and heart tissues isolated from 14Gso mice were fixed in 4% paraformaldehyde and embedded in paraffin blocks using standard techniques. Sections (4–6 μm thickness) were cut and stained with hematoxylin and eosin, PAS/Alcian blue pH 2.5, or used for immunohistochemical analyses as indicated. Immunohistochemical staining was carried out using standard techniques on paraffin embedded sections. Sections were treated with hydrogen peroxide (3% in methanol, RT, >30 min) epitope retrieval solution (Dako) (95°C, 20 min), Proteinase K digested (5 μg/μl, RT, 30 min) and blocked using the BEAT^{TM} method (Zymed). Monoclonal antibodies used anti-carcinoembryonic antigen (Col-1, Zymed) or anti-p53 (PAB1801, Zymed) with incubation of the primary antibody overnight at 4°C and detection with the Picture Plus detection kit with AEC (Zymed). Immunohistochemical staining with polyclonal antibodies to Kcnq1 (H-130, Santa Cruz Biotechnology) was carried out using the HistoMax detection kit with AEC (Zymed).

Stomach pH and acid output was measured as previously described (37) and reported as mean ± SEM. T/T and T/+ groups were compared by *t*-test.

Chromosomal analysis and fluorescent *in situ* hybridization analysis

Chromosomal spreads and karyotype analyses were carried out as previously described (38). BACs chosen from the RPCI-23 or RPCI-24 C57BL/6J mouse BAC libraries were used as templates for the generation of probes for FISH mapping. One microgram of BAC DNA purified using the Plasmid Midi kit (Qiagen) was used in the probe labeling reaction. Probes were labeled using the Nick Translation Kit (Vysis) incorporating SpectrumGreen^{TM} or SpectrumRed^{TM} direct-labeled dUTP (Vysis), ethanol precipitated and resuspended in 45 μl TE. Five microliters of probe, mixed with 5 μg Mouse Cot1 DNA (Invitrogen), was desiccated and resuspended in 10 μl of Kievits hybridization mix (10% dextran sulfate, 2 × SSC, 50% deionized formamide, 0.1% Tween-20 pH 7.0), heated at 60°C, 30 min and pipetted onto previously ethanol dehydrated slides. A coverslip was sealed onto the slide using rubber cement. Slides were heated at 78°C for 5 min and then incubated at 37°C overnight in a humidified box, washed for 2 min in 0.3% Tween-20 in 0.4 × SSC at 73°C, then 1 min in 0.1% Tween-20 in 2 × SSC and rinsed in phosphate buffered saline. Slides were mounted in anti-fade DAPI mounting medium (Vector Laboratories). Probes were protected from light at all times. Slides were visualized on a fluorescent microscope (Zeiss) and the signal analyzed using MacProbe v3.4.1 software (Perceptive Scientific Instruments).

RNA and DNA analysis

RNA was purified using Trizol (Invitrogen) from tissue stabilized in RNALater (Ambion). Reverse transcription was carried out using 1 μg total RNA in a 20 μl reaction using random primers and SuperScript III reverse transcriptase (Invitrogen). Standard PCR amplification in 20 μl reactions was carried out using AmpliTaq DNA polymerase (ABI). PCR conditions were 30 cycles at 94°C, 30 s; 60°C, 30 s; 72°C, 30 s in a PTC-225 thermal cycler (MJResearch). Extension time was increased to 3 min for 3 kb products. Primer sequences are available on request. For Northern analysis, polyA RNA was selected using the PolyATtract mRNA Isolation system (Promega), separated by electrophoresis on a

1% agarose in 0.5 M formaldehyde gel and blotted overnight onto Duralon membrane (Stratagene). The blot was probed with ^{32}P-labeled probes using standard protocols. Signal was detected using the Storm 860 phosphorimager (Molecular Dynamics). The 3′ and 5′ RACE were conducted using the SMART™ RACE cDNA Amplification Kit (BD Biosciences) with nested forward primers in exons 5 and 7 of *Kcnq1* for analysis of 14Gso *Kcnq1* fusion transcript and nested reverse primers in exons 5 and 4 of *Kcnq1* for analysis of *vtg-2* transcript. For sequencing, PCR products were purified from agarose gel using the QiaQuick gel extraction kit (Qiagen) and either sequenced directly or cloned into the pCR2.1 vector by TA cloning (Invitrogen) and sequenced from the plasmid. Sequencing was carried out on an ABI 377 fluorescent sequencer using BigDye Terminator v3.1 chemistry (ABI). PCR for detection of *Helicobacter* was carried out using the method outlined earlier (39); briefly, PCR on DNA purified from stomach tissue was carried out with *Helicobacter* genus specific primers and the product sequenced. The closest match to the observed sequence was found using BLAST on the NCBI nr nucleotide database.

ACKNOWLEDGEMENTS

We thank G. Loots, K. Redding, J. Kim and S. Huntley for critical comments on the manuscript. We also thank G. Wright for the histological analysis on inner ears of 14Gso mice, and A. Petersen and S. Morrison for technical assistance. This work was completed under the auspices of the US Department of Energy, Office of Biological and Environmental Research, by the Lawrence Livermore National Laboratory, University of California, under contract number W-7405-Eng-48.

REFERENCES

1. McColl, K.E., el-Omar, E.M. and Gillen, D. (1997) Alterations in gastric physiology in *Helicobacter pylori* infection: causes of different diseases or all epiphenomena? *Ital. J. Gastroenterol. Hepatol.*, **29**, 459–464.
2. Peek, R.M., Jr and Blaser, M.J. (2002) *Helicobacter pylori* and gastrointestinal tract adenocarcinomas. *Nat. Rev. Cancer*, **2**, 28–37.
3. Obst, B., Wagner, S., Sewing, K.F. and Beil, W. (2000) *Helicobacter pylori* causes DNA damage in gastric epithelial cells. *Carcinogenesis*, **21**, 1111–1115.
4. Naylor, G. and Axon, A. (2003) Role of bacterial overgrowth in the stomach as an additional risk factor for gastritis. *Can. J. Gastroenterol.*, **17** (Suppl. B), 13B–17B.
5. Watanabe, T., Tada, M., Nagai, H., Sasaki, S. and Nakao, M. (1998) *Helicobacter pylori* infection induces gastric cancer in mongolian gerbils. *Gastroenterology*, **115**, 642–648.
6. Lee, A., Fox, J.G., Otto, G. and Murphy, J. (1990) A small animal model of human *Helicobacter pylori* active chronic gastritis. *Gastroenterology*, **99**, 1315–1323.
7. Marchetti, M., Arico, B., Burroni, D., Figura, N., Rappuoli, R. and Ghiara, P. (1995) Development of a mouse model of *Helicobacter pylori* infection that mimics human disease. *Science*, **267**, 1655–1658.
8. Enno, A., O'Rourke, J.L., Howlett, C.R., Jack, A., Dixon, M.F. and Lee, A. (1995) MALToma-like lesions in the murine gastric mucosa after long-term infection with *Helicobacter felis*. A mouse model of *Helicobacter pylori*-induced gastric lymphoma. *Am. J. Pathol.*, **147**, 217–222.
9. Han, S.U., Kim, Y.B., Joo, H.J., Hahm, K.B., Lee, W.H., Cho, Y.K., Kim, D.Y. and Kim, M.W. (2002) *Helicobacter pylori* infection promotes gastric carcinogenesis in a mice model. *J. Gastroenterol. Hepatol.*, **17**, 253–261.
10. Mahler, M., Janke, C., Wagner, S. and Hedrich, H.J. (2002) Differential susceptibility of inbred mouse strains to *Helicobacter pylori* infection. *Scand. J. Gastroenterol.*, **37**, 267–278.
11. Gonzalez, C.A., Sala, N. and Capella, G. (2002) Genetic susceptibility and gastric cancer risk. *Int. J. Cancer*, **100**, 249–260.
12. Nardone, G. (2003) Review article: molecular basis of gastric carcinogenesis. *Aliment. Pharmacol. Ther.*, **17** (Suppl. 2), 75–81.
13. Sundt, T.M., III, Compton, C.C. and Malt, R.A. (1988) Menetrier's disease. A trivalent gastropathy. *Ann. Surg.*, **208**, 694–701.
14. Reinhardt, J.D., McCloy, R.M. and Blackwell, C.F. (1976) Autoimmune atrophic gastritis with hypergastrinemia. *South Med. J.*, **69**, 1551–1553.
15. Lee, M.P., Ravenel, J.D., Hu, R.J., Lustig, L.R., Tomaselli, G., Berger, R.D., Brandenburg, S.A., Litzi, T.J., Bunton, T.E., Limb, C. *et al.* (2000) Targeted disruption of the *Kvlqt1* gene causes deafness and gastric hyperplasia in mice. *J. Clin. Invest.*, **106**, 1447–1455.
16. Dedek, K. and Waldegger, S. (2001) Colocalization of KCNQ1/KCNE channel subunits in the mouse gastrointestinal tract. *Pflugers Arch.*, **442**, 896–902.
17. Grahammer, F., Herling, A.W., Lang, H.J., Schmitt-Graff, A., Wittekindt, O.H., Nitschke, R., Bleich, M., Barhanin, J. and Warth, R. (2001) The cardiac K+ channel KCNQ1 is essential for gastric acid secretion. *Gastroenterology*, **120**, 1363–1371.
18. Neyroud, N., Tesson, F., Denjoy, I., Leibovici, M., Donger, C., Barhanin, J., Faure, S., Gary, F., Coumel, P., Petit, C. *et al.* (1997) A novel mutation in the potassium channel gene *KVLQT1* causes the Jervell and Lange–Nielsen cardioauditory syndrome. *Nat. Genet.*, **15**, 186–189.
19. Splawski, I., Timothy, K.W., Vincent, G.M., Atkinson, D.L. and Keating, M.T. (1997) Molecular basis of the long-QT syndrome associated with deafness. *N. Engl. J. Med.*, **336**, 1562–1567.
20. Wang, Q., Curran, M.E., Splawski, I., Burn, T.C., Millholland, J.M., VanRaay, T.J., Shen, J., Timothy, K.W., Vincent, G.M., de Jager, T. *et al.* (1996) Positional cloning of a novel potassium channel gene: KVLQT1 mutations cause cardiac arrhythmias. *Nat. Genet.*, **12**, 17–23.
21. Scarff, K.L., Judd, L.M., Toh, B.H., Gleeson, P.A. and Van Driel, I.R. (1999) Gastric H(+),K(+)-adenosine triphosphatase beta subunit is required for normal function, development, and membrane structure of mouse parietal cells. *Gastroenterology*, **117**, 605–618.
22. Spicer, Z., Miller, M.L., Andringa, A., Riddle, T.M., Duffy, J.J., Doetschman, T. and Shull, G.E. (2000) Stomachs of mice lacking the gastric H,K-ATPase alpha-subunit have achlorhydria, abnormal parietal cells, and ciliated metaplasia. *J. Biol. Chem.*, **275**, 21555–21565.
23. Franic, T.V., Judd, L.M., Robinson, D., Barrett, S.P., Scarff, K.L., Gleeson, P.A., Samuelson, L.C. and Van Driel, I.R. (2001) Regulation of gastric epithelial cell development revealed in H(+)/K(+)-ATPase beta-subunit- and gastrin-deficient mice. *Am. J. Physiol. Gastrointest. Liver Physiol.*, **281**, G1502–G1511.
24. Sharp, R., Babyatsky, M.W., Takagi, H., Tagerud, S., Wang, T.C., Bockman, D.E., Brand, S.J. and Merlino, G. (1995) Transforming growth factor alpha disrupts the normal program of cellular differentiation in the gastric mucosa of transgenic mice. *Development*, **121**, 149–161.
25. Gut, M.O., Parkkila, S., Vernerova, Z., Rohde, E., Zavada, J., Hocker, M., Pastorek, J., Karttunen, T., Gibadulinova, A., Zavadova, Z. *et al.* (2002) Gastric hyperplasia in mice with targeted disruption of the carbonic anhydrase gene *Car9*. *Gastroenterology*, **123**, 1889–1903.
26. Aly, A., Shulkes, A. and Baldwin, G.S. (2004) Gastrins, cholecystokinins and gastrointestinal cancer. *Biochim. Biophys. Acta*, **1704**, 1–10.
27. Baldus, S.E., Monig, S.P., Arkenau, V., Hanisch, F.G., Schneider, P.M., Thiele, J., Holscher, A.H. and Dienes, H.P. (2002) Correlation of MUC5AC immunoreactivity with histopathological subtypes and prognosis of gastric carcinoma. *Ann. Surg. Oncol.*, **9**, 887–893.
28. Velcich, A., Yang, W., Heyer, J., Fragale, A., Nicholas, C., Viani, S., Kucherlapati, R., Lipkin, M., Yang, K. and Augenlicht, L. (2002) Colorectal cancer in mice genetically deficient in the mucin Muc2. *Science*, **295**, 1726–1729.
29. Byrd, J.C., Yunker, C.K., Xu, Q.S., Sternberg, L.R. and Bresalier, R.S. (2000) Inhibition of gastric mucin synthesis by *Helicobacter pylori*. *Gastroenterology*, **118**, 1072–1079.

30. Morgenstern, S., Koren, R., Moss, S.F., Fraser, G., Okon, E. and Niv, Y. (2001) Does *Helicobacter pylori* affect gastric mucin expression? Relationship between gastric antral mucin expression and *H. pylori* colonization. *Eur. J. Gastroenterol. Hepatol.*, **13**, 19–23.
31. Stubbs, L., Carver, E.A., Cacheiro, N.L., Shelby, M. and Generoso, W. (1997) Generation and characterization of heritable reciprocal translocations in mice. *Methods*, **13**, 397–408.
32. Frohman, M.A. (1993) Rapid amplification of complementary DNA ends for generation of full-length complementary DNAs: thermal RACE. *Methods Enzymol.*, **218**, 340–356.
33. Casimiro, M.C., Knollmann, B.C., Ebert, S.N., Vary, J.C., Jr, Greene, A.E., Franz, M.R., Grinberg, A., Huang, S.P. and Pfeifer, K. (2001) Targeted disruption of the *Kcnq1* gene produces a mouse model of Jervell and Lange–Nielsen Syndrome. *Proc. Natl Acad. Sci. USA*, **98**, 2526–2531.
34. Schmitt, N., Schwarz, M., Peretz, A., Abitbol, I., Attali, B. and Pongs, O. (2000) A recessive C-terminal Jervell and Lange–Nielsen mutation of the KCNQ1 channel impairs subunit assembly. *EMBO J.*, **19**, 332–340.
35. Tyson, J., Tranebjaerg, L., McEntagart, M., Larsen, L.A., Christiansen, M., Whiteford, M.L., Bathen, J., Aslaksen, B., Sorland, S.J., Lund, O. *et al.* (2000) Mutational spectrum in the cardioauditory syndrome of Jervell and Lange–Nielsen. *Hum. Genet.*, **107**, 499–503.
36. Stolte, M. and Eidt, S. (1989) Lymphoid follicles in antral mucosa: immune response to *Campylobacter pylori*? *J. Clin. Pathol.*, **42**, 1269–1271.
37. Gut, M.O., Parkkila, S., Vernerova, Z., Rohde, E., Zavada, J., Hocker, M., Pastorek, J., Karttunen, T., Gibadulinova, A., Zavadova, Z., Knobeloch, K.P., Wiedenmann, B., Svoboda, J., Horak, I., Pastorekova, S. (2002) Gastric hyperplasia in mice with targeted disruption of the carbonic anhydrase gene *Car9*. *Gastroenterology*, **123**, 1889–1903.
38. Chittenden, L., Lu, X., Cacheiro, N.L., Cain, K.T., Generoso, W., Bryda, E.C. and Stubbs, L. (2002) A new mouse model for autosomal recessive polycystic kidney disease. *Genomics*, **79**, 499–504.
39. Riley, L.K., Franklin, C.L., Hook, R.R., Jr and Besch-Williford, C. (1996) Identification of murine helicobacters by PCR and restriction enzyme analyses. *J Clin. Microbiol.*, **34**, 942–946.